Advances in Materials Research, *Vol. 10*, *No. 4* (*2021*) *331-341*
https://doi.org/10.12989/amr.2021.10.4.331

Manufacture of Al_2O_3/Ti composite by aluminum bonding reaction for their use as a biomaterial

Ruth P. Alvarez-Carrizal [1], José A. Rodríguez-García [1], Dora A. Cortés-Hernández [2], Sergio J. Esparza-Vázquez [1] and Enrique Rocha-Rangel [*1]

[1] *Research Department*, *Universidad Politécnica de Victoria*, *Av. Nuevas Tecnologías 5902*, *Ciudad Victoria*, *Tamaulipas*, *87138*, *México*
[2] *Cinvestav-Saltillo*, *Avenida Industria Metalurgica1062*, *Parque Industrial Saltillo-Ramos Arizpe*, *Ramos Arizpe*, *Coahuila*, *25900*, *México*

(*Received February 2*, *2021*, *Revised October 27*, *2021*, *Accepted October 28*, *2021*)

Abstract. This research shows the development of a composite material with an alumina matrix reinforced with different percentages of titanium (0.0%, 0.5%, 1%, 2% y 3%) with the intention of analyzing their mechanical and biocompatible properties for its possible application as a biomaterial. Alumina was synthesized using the reaction bonding aluminum oxide (RBAO) methodology. The powders resulting from the milling process had a size distribution ranging from nanometers to 2 microns. By means of X-ray diffraction and differential thermal analysis, it was determined that aluminum oxidizes in both solid and liquid states. It was also found that the alumina formation reaction is complete at 900°C. Using scanning electron microscopy, it was determined that the microstructure has fine grain sizes and homogeneous morphology. Likewise, the elastic modulus and fracture toughness of the composites obtained were determined, results indicate that these properties are higher than the properties of cortical bone. In addition, bioactivity was promoted using the biomimetic method. The results obtained demonstrate that the resulting composite can be used as a biomaterial.

Keywords: Al_2O_3/Ti composite; bioactivity; biomaterial; bone implants; RBAO process

1. Introduction

There are several composites currently used as biomaterials, which can be made of different matrices. However, the most widely used is the ceramic matrix, since it provides high biocompatibility, hardness and good wear and corrosion resistance (Wintermantel *et al*. 2001). Today, one of the most widely used ceramics as a matrix for composite materials is alumina (Al_2O_3), since this compound shows no deformation under the action of a load, due to its high elastic modulus, which makes it suitable for obtaining new materials with combinations of properties due to its ease homogeneous incorporation of fine particles into its matrix (Konopka 2015). In addition, it has been demonstrated that this material has good properties as a biomaterial (Saini *et al*. 2015), being mainly used as a matrix in composite materials in osteosynthesis, arthroplasty and as friction and osteoconduction surfaces (Xifré-Pérez *et al*. 2015).

*Corresponding author, Ph.D., E-mail: erochar@upv.edu.mx

 ISSN: 2234-0912 (Print), 2234-179X (Online)

The effect of the addition of metallic particles to alumina matrices has been extensively studied, and there are several metallic materials that can be added as reinforcements (Rocha-Rangel *et al*. 2019). Titanium is one of the most commonly used biomaterials for the fabrication of prostheses and bone implants, as it has excellent mechanical tensile strength, fatigue resistance, ductility and toughness (Quinn *et al*. 2020).

It is therefore believed to be a good reinforcement in alumina matrices, as it has been reported that the titanium content in cermet directly affects the densification of the composite, which in turn causes positive effects on the hardness and toughness of the composite. Both elements (alumina and titanium) are considered materials compatible with the human body, therefore, if Al_2O_3/Ti cermets are manufactured with adequate microstructure and mechanical properties, the resulting material may have a use as a biomaterial (Guzman *et al*. 2016). Some researchers have proposed fabricating composites with potential applications as biomaterials in prostheses and bone implants, such as Oshkour, who studied the mechanical properties of Calcium Silicate with Ti-55Ni and Ti-6Al-4V Alloys for hard tissues replacement (Ataollahi Oshkour *et al*. 2014). More recently, Al_2O_3/Ti functionally graded material was proposedw for its use in orthopedic applications (Bahraminasab *et al*. 2017). On the other hand, alternative methods involving slow drug delivery systems have also been studied in order to alleviate postoperative infections caused by orthopedic implants, such is the case of the study conducted by Karacan (Karacan *et al*. 2019), in which untreated, thermally anodized Ti6Al4V disks coated with polylactic acid (PLA) containing gentamicin and antibiotic-loaded coralline hydroxyapatite, in order to reduce the risk of postoperative infections due to implants with biomaterials. A further study showed that Poly (butylene adipate-co-terephilate) based materials with various percentages of wollastonite (0 to 7%wt) manufactured by the molten-state process showed potential benefits that can be exploited for their application as biomaterials in the field of biomedicine (Bheemaneni *et al*. 2018). Maji and Choubey (2018) carried out a work in which they used a matrix of very fine zirconia particles reinforced with aluminum, based on their results it was determined that the composite obtained can be used in different biomedical and orthopedic applications. Another study involved the use of composite materials of various matrices, mainly ceramic, for use in maxillary sinus augmentation procedures on immediate or delayed osseo integrated implants, does not generate anaphylactic reactions in patients and can be used with the different surgical techniques without any complication (Scharager-Lewin *et al*. 2016). Thus, from the bibliographic review carried out, it was observed that the Al_2O_3/Ti system has been little studied, so that the goal of this work is to fabricate Al_2O_3/Ti composites by oxidation-sintering methods to determine their possible application as bone implants in living beings.

2. Experimental

Alumina-titanium composites were manufactured by the powder technique, using the following raw materials: titanium (Aldrich, purity: 99.99%, 5-10 μm), aluminum (Aldrich, purity: 99.99%, 5-10 μm) and alumina (Aldrich, purity: 99.99%, 1 μm). The 30% of the alumina used for the preparation of composites was synthesized using the RBAO process, method used to obtain nanometric Al_2O_3 particles from the oxidation of metallic Al and thus obtaining the advantages of the formation of an oxide from the oxidation of a metal (Claussen *et al*. 1994). The grinding of the powders was carried out in two stages, in the first (oxidizing stage) only the Al + Al_2O_3 mixture was ground. The second milling was carried out with the powders resulting from the oxidizing

stage plus Ti aggregates. In order to determine the effect of Ti on the mechanical and chemical properties of Al_2O_3, titanium was added in the alumina matrix in proportions of 0, 0.5, 1, 2 and 3 wt.%. Each mixture of different composition was subjected to a high-energy milling process (Fritsch, Pulviressete 6), using isopropyl alcohol as control agent, ZrO_2 spherical grinding media, keeping a grinding ratio of 20:1, during 3 h at 300 rpm. After the grinding of the powders, their size and particle size distribution were determined with a Mastersizer 2000, England equipment. To follow the transformation sequence of the reagents (Al + Al_2O_3) after first grinding, interrupted tests were carried out in an electric furnace (Thermo Scientific Thermolyne FB1315M, USA) at different temperature (450, 600, 750, 900 y 1100°C), at atmospheric pressure. For this purpose, powders were heated at a speed of 2°C/min to the desired temperature and cooled down inside the furnace. After heating, all powders were analyzed by X-ray diffraction (Panalytical x'pert pro, Japan) to determine the crystalline species present. To follow the progress of reaction 1, a sample of the first powder mixture is subjected to thermogravimetric analysis in a Shimadzu, DTG-60-H, Japan equipment. With the powders resulting from the second grinding stage, cylindrical tablets 2 cm in diameter by 0.3 cm thick were obtained by uniaxial compaction at 350 MPa using a press (Porter-30T, Mexico), which were then subjected to sintering treatments during 2 h at 1500°C in an electric furnace. To determine the crystalline phases of the formed composite, an X-ray diffraction study was carried out. For the identification of the diffraction peaks, the obtained diffractograms were compared with the charts available in the PCPDFWIN database. Fracture toughness was obtained by the indentation fracture technique using the Miyoshi's equation (Miyoshi *et al*. 1985). Finally, the microstructure was analyzed by scanning electron microscopy (JEOL, JSM6400).

$$2Al + 3/2O_2 + Al_2O_{3(\text{seed-old alumina})} \rightarrow Al_2O_{3(\text{new alumina})} \quad (1)$$

The re-immersion method was used to promote bioactivity on the composites. The solutions were prepared according to what Kokubo mentions in his publications (Kokubo *et al*. 1990), using two simulated biological fluids, one with an ionic concentration similar to that of human blood plasma (SBF) and the other 40% more concentrated (1.4SBF).

3. Results

3.1 Particle size distribution

During the milling process, very fine particle powders of different sizes were obtained, as shown in Fig. 1, where it is found that approximately 30% of the powders have sizes smaller than 1 μm. About 50% of the powders have a particle size between 1-2 μm, and the remaining 20% have sizes greater than 2 μm, which do not reach 3 μm. The average particle size was 1.34 μm. It is worth mentioning that 30% of the powders have nanometer sizes indicating that the mechanical milling and RBAO process were satisfactory. This fine particle size favours the sintering process, since the increase in surface area favours the contact between particles, which in turn allows higher densification and thus an improvement in the mechanical properties of the composites obtained.

3.2 Thermogravimetric analysis

A thermogravimetric analysis was performed on the powders resulting from the first milling in

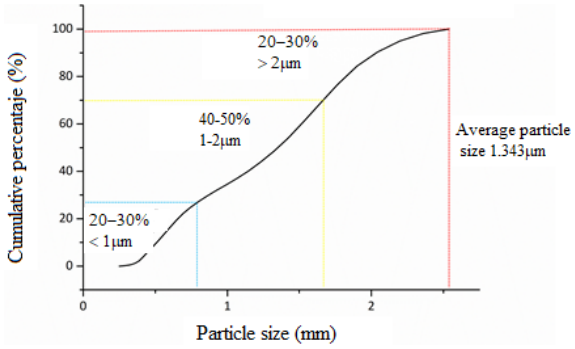

Fig. 1 Powder particle size

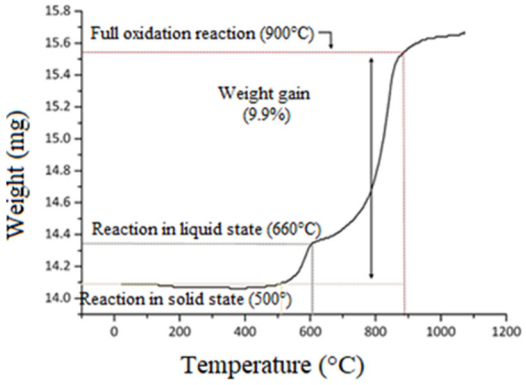

Fig. 2 Monitoring of the Al oxidation reaction by thermogravimetric analysis

order to follow the sequence of aluminum oxidation (Fig. 2). This figure shows that from the beginning of the process and up to 500° there was no change in the weight of the sample. However, from this point on, a slight gain in weight begins due to the start of the aluminum oxidation reaction, which at this temperature is still in the solid state, when reaching the temperature of 660°, aluminum reaches its melting temperature, and it is here where there begins to be a considerable gain in weight because aluminum oxidizes more easily in the liquid state. Complete oxidation reaction ends at 900°C. Thus, from the beginning of the reaction until its completion, there was a weight gain of 9.9%, which corresponds to the introduction of oxygen to the sample by the oxidation of aluminum to form new alumina (RBAO process).

3.3 X-ray diffraction (*Interrupted tests*)

The progress of the aluminum oxidation reaction (RBAO process) was also monitored by X-ray diffraction. Fig. 3 shows the diffraction patterns of samples subjected to interrupted heating tests at different temperatures. In pattern (a-450°C), there are particles of both alumina and aluminum distributed throughout the sample. As it can be observed in pattern (b-600°C), the intensity of the aluminum peaks is decreasing, this is because it begins to transform into alumina. As shown in pattern (c-750°C), this transformation continues to be observed, until reaching almost the culmination of the reaction in the pattern (d-900°C), where only a small aluminum peak can be

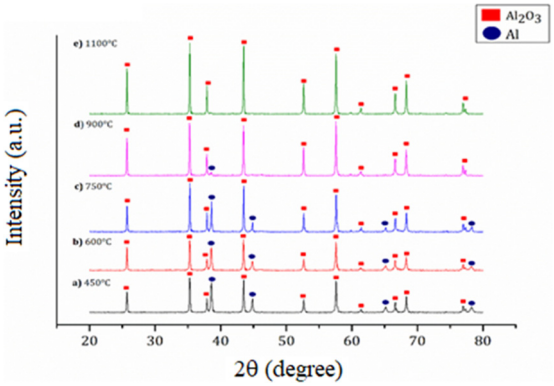

Fig. 3 X-ray diffraction patterns in interrupted tests. a) 450°C test; b) 600°C test; c) 750°C test; d) 900°C test; e) 1100°C test

seen. Finally, in pattern (e-1100°C), it can be seen how the aluminum oxidation reaction was successfully carried out, since there was only alumina in the sample.

3.4 Microstructural analysis

Fig. 4 shows the micrographs obtained by Scanning Electron Microscopy, which correspond to the samples sintered at 1500°C with aggregates of 0.05%, 1%, 2% and 3%. In general, it can be observed that the microstructure presents irregularly shaped grains, with sizes smaller than 20 µm. When comparing the microstructures, it is possible to observe that the titanium content has an important effect on the microstructure, since the samples with a higher titanium addition present an

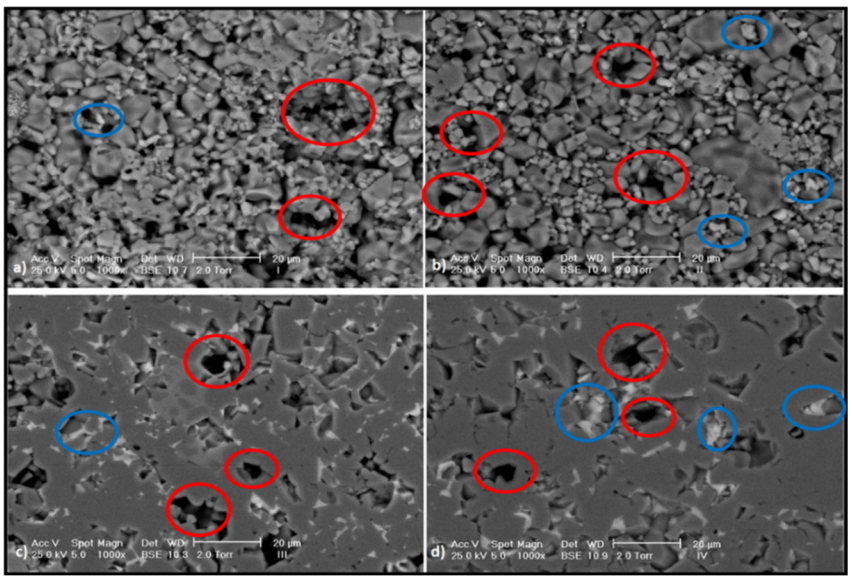

Fig. 4 Scanning electron microscopy performed on each of the samples. a) Al_2O_3 +0.5%Ti; b) Al_2O_3 +1%Ti; c) Al_2O_3 +2%Ti; d) Al_2O_3 +3%Ti

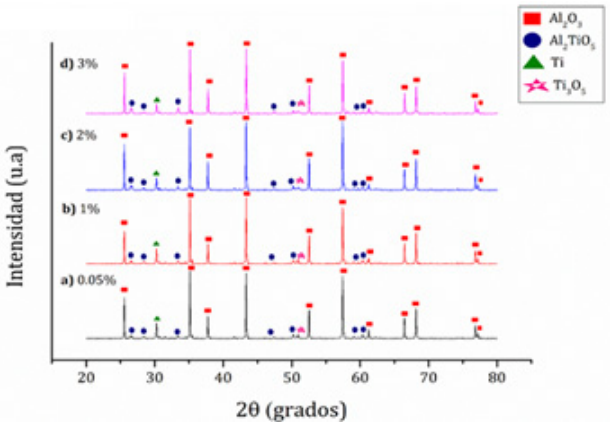

Fig. 5 Diffraction patterns of samples sintered at 1500°C for 2 h. a) Al_2O_3 +0.5%Ti; b) Al_2O_3 +1%Ti; c) Al_2O_3 +2%Ti; d) Al_2O_3 +3%Ti

agglomeration of the grains, as it can be seen in micrographs c and d, which show samples that contain titanium aggregates of 2% and 3%, respectively. On the other hand, it can also be observed in the micrographs the presence of porosity, which was also observed in the alumina matrix, which indicates that this porosity is given by the alumina present in the samples and this property may favor the growth of a bioactive agent, this can be seen in micrographs a and b, corresponding to the 0.05% and 1% Ti aggregates, which are the ones with the highest porosity. The circles in red show the areas with higher porosity, which are shown in black in the micrograph. Another important characteristic that can also be noticed in these micrographs is the presence of titanium, which can be observed as small white grains. In the first samples corresponding to the 0.05% and 1% aggregates (a and b), they appear only as grains, as shown in the image below (blue circles). As the percentage of titanium increases, so does its appearance, but, in these last two micrographs, it appears more as an agglomerate in certain areas of the sample.

3.5 X-ray diffraction (Sintered samples)

Fig. 5 shows the diffraction patterns of samples sintered at 1500°C for 2 h, with titanium aggregates at 0.05%, 1%, 2% and 3%. The main crystalline phase observed is alumina (Al_2O_3), the explanation for its presence is that this is the matrix in each of the samples. The next compound that appears is aluminum titanate (Al_2TiO_5), present in each of the patterns, which is due to the fact that during the sintering treatment some oxidation of the titanium powder added to each of the samples occurred, thus forming titanium oxide (TiO_2), which, in the presence of alumina, forms Al_2TiO_5. As mentioned above, sintering was carried out in a controlled nitrogen atmosphere to avoid oxidation of the titanium, however, as we have already seen, given the results of these patterns, this was not possible. Nevertheless, the presence of metallic titanium in the sample can be observed.

3.6 Mechanical properties

3.6.1 Elastic modulus and fracture toughness

Fig. 6 shows a plot of the elastic modulus as a function of the titanium aggregates contained in

each sample. As it can be seen, the highest value for the elastic modulus is found in the control sample, and although what is sought is that the value of this property is higher in titanium aggregates, it does not mean that they cannot be used as biomaterial, the values for the elastic modulus of the femur range between 205-208 GPa, which indicates that any of the aggregates to be used as biomaterial for an application similar to that of the femur can be used, taking into account that, of these four aggregates, the one with the best elastic modulus is the one containing 0.05% aggregate, however, it is also important to mention that, as the titanium content in the sample increases, the value for the elastic modulus decreases. Considering then that the elastic modulus measures the resistance of the material to deformation, it follows that samples with a higher value of elastic modulus will have a higher resistance to deformation. Fig. 6 also shows the results corresponding to the fracture toughness measurements of each of the samples sintered at 1500°C for 2 h. One of the most important observations that can be made in the graph, firstly, is that the values with titanium aggregates are higher than those of the control sample. It can also be observed that the highest value for fracture toughness is found in the 1% aggregate, taking into account that the minimum that should be presented compared to the femur mentioned above, given the characteristics of biomaterial to be taken from the samples, should be 5.6 $MPam^{1/2}$, and the only one that presents this characteristic is the 1% aggregate, however, the other samples show a value for fracture toughness equal to or slightly lower than that of this bone.

3.7 X-ray diffraction (*Bioactivity*)

To promote bioactivity of samples with the different titanium aggregates, the biomimetic method was used in which the bioactivity of the compound was demonstrated by the immersion route with the use of a bioactive agent (wollastonite). The evolution of the bioactivity of the sample was demonstrated by X-ray diffraction, where it can be seen how the immersion of the composites in SBF and 1.4SBF favors the formation of hydroxyapatite. Fig. 7 shows the evolution of the samples for 7, 14 and 21 days of testing. In the first 7 days, high peaks corresponding to Ca can be observed in each of the patterns, this is due to the fact that, in the first stage, each of the

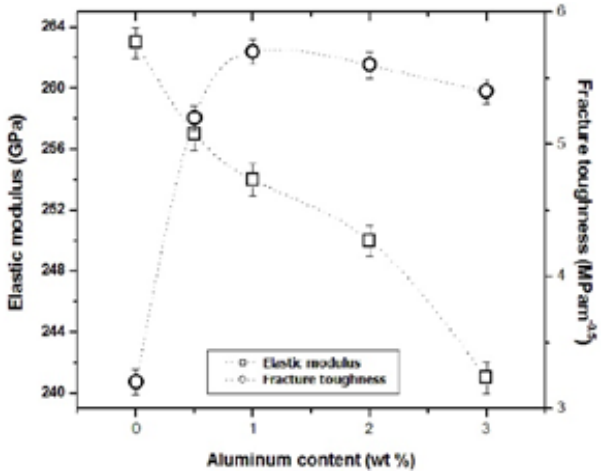

Fig. 6 Elastic modules and fracture toughness of samples sintered at 1500°C for 2 h. The elastic modulus and fracture toughness of a femur bone is 206 MPa and 5.6 $MPam^{1/2}$ respectively

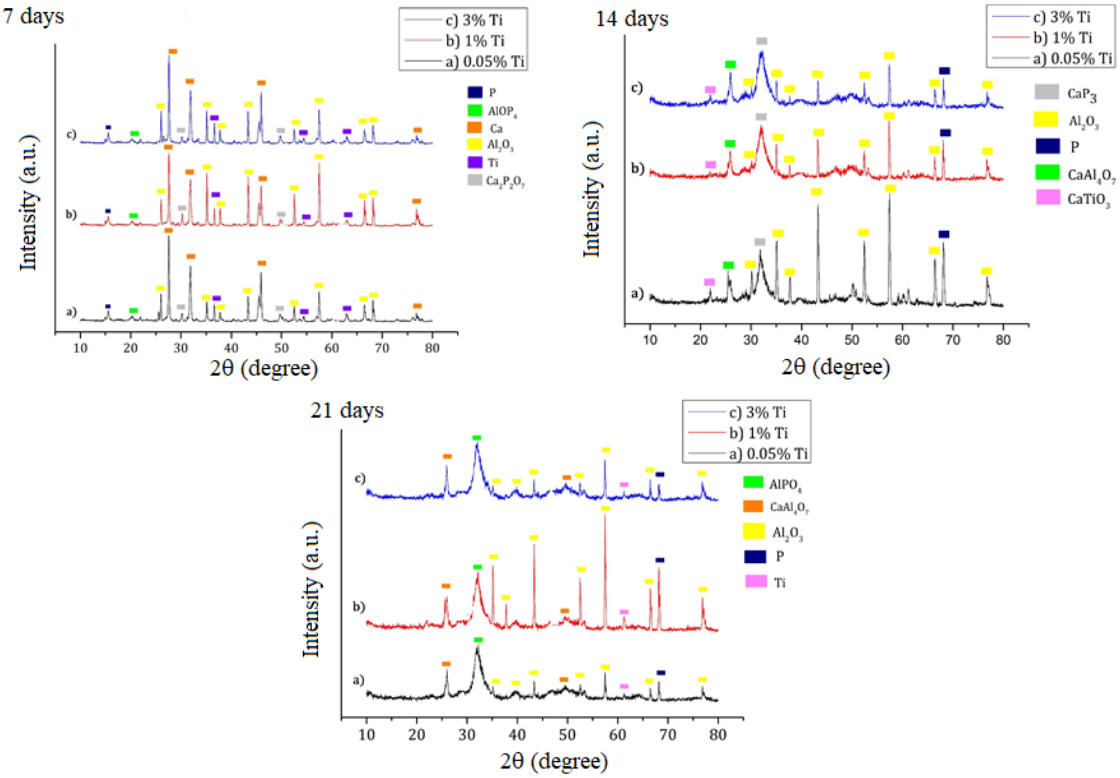

Fig. 7 Biomimetic method, stage 1 (7 days), stage 2 (14 days) and stage 3 (21 days). a) Al_2O_3+0.5%Ti; b) Al_2O_3+1%Ti; c) Al_2O_3+3%Ti

samples has a light bed of wollastonite ($CaSiO_3$), which is why, when interacting with the sample and with the fluid, be reactions between these two components start. It can also be observed that the first peak, in each of the standards with samples at 0.05%, 1% and 3%, is phosphorus (P). The occurrence of this element is quite important, as there is an indication of the formation of hydroxyapatite, which is the indication that the composite can be called a bioactive material. Hydroxyapatite (HA) appears in the composites, forming a light layer on them, which will allow bone regeneration. It is also important to mention the formation of some other compounds such as $Ca_2P_2O_7$ or $AlOP_4$, due to the interaction between the samples, the solution and the wollastonite bed.

As mentioned above, the formation of hydroxyapatite ($Ca_5(PO_4)_3(OH)$) is really important, as it shows that the composite is bioactive. We can observe this in the next stage of the biomimetic method (14 days). Here we can already observe a decrease in calcium as an individual compound, but there are more components that include it, as well as phosphorus, which indicates the formation of hydroxyapatite.

As the study progressed, the permanence of phosphorus, an indicator of the presence of hydroxyapatite, can be seen. In the Fig. 7 (21 days), it can be seen that the pattern having a higher intensity of this element is the sample with 1% Ti (item b). The formation of different compounds can also be observed, which, as mentioned, are the result of the interactions between the fluid components and the alumina matrix samples with titanium aggregates in different percentages.

Table 1 Chemical composition of remaining fluids of biomimetic method by AA and ICP

Sample	Ca (mg/l)	P (mg/l)	Al (mg/l)	Ti (mg/l)
1	70.64	36.30	< 0.10	< 0.10
2	72.48	15.14	< 0.10	< 0.10
3	91.02	46.44	< 0.10	< 0.10
4	354.80	< 0.10	< 0.10	< 0.10
5	564.7	< 0.10	< 0.10	< 0.10
6	585.20	< 0.10	< 0.10	< 0.10
7	545.20	< 0.10	< 0.10	< 0.10
8	557.30	< 0.10	< 0.10	< 0.10
9	596.20	< 0.10	< 0.10	< 0.10
10	540.20	< 0.10	< 0.10	< 0.10
11	573.80	< 0.10	< 0.10	< 0.10
12	590.40	< 0.10	< 0.10	< 0.10
13	92.09	0.211	< 0.10	< 0.10
14	90.20	0.374	< 0.10	< 0.10
15	88.18	0.516	< 0.10	< 0.10
16	91.01	0.508	< 0.10	< 0.10
17	134.0	< 0.10	< 0.10	< 0.10
18	93.40	< 0.10	< 0.10	< 0.10
19	63.29	27.66	< 0.10	< 0.10
20	52.69	28.50	< 0.10	< 0.10
21	6.14	27.46	< 0.10	< 0.10
22	70.43	35.35	< 0.10	< 0.10

This can be demonstrated by means of an Absorption Spectroscopy (AA) and Plasma Atomic Emission Spectroscopy (ICP) study, carried out in an atomic absorption equipment Thermo Scientific model ICE 3300 and a plasma emission spectrometer Perkin Elmer Model Optima 8300. Using this study, it is possible to determine the amount of each of the elements present only in the fluid remaining in the samples.

In Table 1, 1 corresponds to the initial SBF. Samples 2 and 3 correspond to the concentrated SBF at 1.4%). Samples 4-12 correspond to the fluids with unconcentrated SBF. Samples 4-6 (7 days), 7-9 (14 days) and 10-12 (21 days) correspond to the 0.05%, 1% and 3% titanium tablets, respectively. Once the first stage was completed, the liquid is removed from all samples by changing the liquid to 1.4SBF. Samples 13-18 correspond to the second immersion stage (7 days). Sample 13-15 (14 days) with titanium aggregates of 0.05%, 1% and 3% respectively. Once the 14 days had passed, the liquid and tablets were removed. Samples 16-18 are from the third system (21 days). Samples 19-22 is the last liquid corresponding to the last stage corresponding to the re-immersion (liquid is returned to 1.4%). Table 1 shows the main components present in each of the samples. From this, we can observe that in samples 1-3 a moderate amount of calcium and phosphorus is observed, due to the presence of the wollastonite bed. In the following samples 4-10, we see a large presence of calcium, but no phosphorus, and it is in this transition period of 7-14

days, in which there begins to be a proliferation of phosphorus. From samples 11-22, we again see the presence of calcium and phosphorus, since there is already beginning to be an activation of the material, allowing the growth of hydroxyapatite, which is why there is beginning to be an amount of calcium and phosphorus. Although, the amounts are not as large as those at the beginning, their presence is important, as they indicate growth on the surface of the sample, which is more important. It is also significant to note that the amounts of aluminum and titanium are quite low, since most of them are present in the samples and not in the fluids.

4. Conclusions

- Micrometer-scale particles of alumina were obtained as a result of the mechanical milling process and the RBAO process, with an average size of 1,343 μm.
- There was an increase in the mechanical properties of the composite, having that, the best option, for the desired application is the composite that has titanium aggregates in 1%, considering that, a comparison was made with the femur.
- The titanium content has a direct effect on the properties of porosity, hardness and fracture toughness, and although most of the composites formed have an increase in these mechanical properties, it is important to highlight that the best material will have the best properties considering the possible application that will be given to it.
- The use of the biomimetic method for bioactivation of a composite material is feasible after 21 days, when hydroxyapatite begins to proliferate on the surface of the substrates.
- It is possible to use powder techniques to obtain alumina-based composites with high fracture toughness values, combined with the application of the biomimetic method for the bioactivation of the material, making possible its application as a bone substitute or implant.

References

Ataollahi Oshkour, A., Pramanik, S., Shirazi, S.F.S., Mehrali, M., Yau, Y.H. and Abu Osman, N.A. (2014), "A comparison in mechanical properties of cermets of calcium silicate with Ti-55Ni and Ti-6Al-4V alloys for hard tissues replacement", *Scientif. World J.*, **2014**, 616804. https://doi.org/10.1155/2014/616804

Bahraminasab, M., Ghaffari, S. and Eslami-Shahed, H. (2017), "Al_2O_3-Ti functionally graded material prepared by spark plasma sintering for orthopaedic applications", *J. Mech. Behav. Biomed. Mater.*, **72**, 82-89. https://doi.org/10.1016/j.jmbbm.2017.04.024

Bheemaneni, G., Saravana, S. and Kandaswamy, R. (2018), "Processing and characterization of poly (butylene adipate-co-terephthalate) / wollastonite biocomposites for medical applications", *Materials Today*: *Proceedings*, **5**(1), 1807-1816. https://doi.org/10.1016/j.matpr.2017.11.279

Claussen, N., Wu, S. and Holz, D. (1994), "Reaction bonding of aluminum oxide (RBAO) composites: processing, reaction mechanisms and properties", *J. Eur. Ceram. Soc.*, **14**(2), 97-109. https://doi.org/10.1016/0955-2219(94)90097-3

Guzman, R., Fernández-García, E., Gutiérrez-González, C.F., Fernández, Adolfo., López-Lacomba, J. L. and López-Esteban, S. (2016), "Biocompatibility assessment of spark plasma-sintered alumina-titanium cermets", *J. Biomater. Applicat.*, **30**(6), 759-769. https://doi.org/10.1177/0885328215584858

Karacan, I., Ben-Nissan, B., Wang, H.A., Juritza, A., Swain, M.V., Müller, W.H., Chou, J., Stamboulis, A., Macha, I.J. and Taraschi, V. (2019), "Mechanical testing of antimicrobial biocomposite coating on metallic medical implants as drug delivery system", *Mater. Sci. Eng. C*, **104**, 109757. https://doi.org/10.1016/j.msec.2019.109757

Kokubo, T., Kushitani, H., Sakka, S., Kitsugi, T. and Yamamuro, T. (1990), "Solutions able to reproduce in

vivo surface-structure changes in bioactive glass-ceramic A-W3", *J. Biomed. Mater. Res.*, **24**(6), 721-734. https://doi.org/10.1002/jbm.820240607

Konopka, K. (2015), "Alumina composites with metal particles in ceramic matrix", *Powder Metall. Metal Ceram.*, **54**, 374-379. https://doi.org/10.1007/s11106-015-9724-5

Maji, A. and Choubey, G. (2018), "Microstructure and mechanical properties of alumina toughened zirconia (ATZ)", *Materials Today*: *Proceedings*, **5**(2), 7457-7465. https://doi.org/10.1016/j.matpr.2017.11.417

Miyoshi, T., Sagawa, N. and Sassa, T. (1985), "Study on fracture toughness evaluation for structural ceramics", *Transact. Japan Soc. Mech. Eng.*, **51**, 2489-2497. https://doi.org/10.1299/kikaia.51.2489

Quinn, J., McFadden, R., Chan, C.W. and Carson, L. (2020), "Titanium for orthopaedic applications: an overview of surface modification to improve biocompatibility and prevent bacterial biofilm formation", *Science*, **23**(11), 101745. https://doi.org/10.1016/j.isci.2020.101745

Rocha-Rangel, E., López-Hernández, J., Calles-Arriaga, C.A., Pech-Rodríguez, W.J., Armendáriz-Mireles, E.N., Castillo-Robles, J.A. and Rodríguez-García, J.A. (2019), "Effect of additions of metal sub-micron particles on properties of alumina matrix composites", *J. Mater. Res.*, **34**, 2983-2989. https://doi.org/10.1557/jmr.2019.178

Saini, M., Singh, Y., Arora, P., Arora, V. and Jain, K. (2015), "Implant biomaterials: A comprehensive review", *World J. Clinical Cases*, **3**(1), 52-57. https://doi.org/10.12998/wjcc.v3.i1.52

Scharager-Lewin, D., Arraño-Scharager, D.P. and Biotti-Picand, J. (2016), "Biomateriales en levantamiento de seno maxilar para implantes dentales", *Revista Clínica Periodoncia*, *Implantología y Rehabilitación Oral*, **10**(1), 20-25. https://doi.org/10.1016/j.piro.2016.06.002

Wintermantel E., Mayer, J. and Goehring, T.N. (2001), "Composites for Biomedical Applications", *Encyclopedia of Materials*: *Science and Technology*, 1371-1376.

Xifre-Perez, E., Ferre-Borull, J., Pallares, J. and Marsal, L.F. (2015), "Mesoporous alumina as a biomaterial for biomedical applications", *Mesoporous Biomater.*, **2**, 13-32. https://doi.org/10.1515/mesbi-2015-0004

CH